



Simultaneous Photodegradation and Removal of Organic-Inorganic Pollutants over Zeolite Prepared from Saudi Arabia Kaolin

Islam Hamdy Abd El Maksod^{1,2}, Samia Abdel Hmeed Kosa² and Hanan Kharman El Zahrani², Eman Zakaria Hussein Hegazy^{1,2*}

¹National Research Centre (NRC), Dokki, Cairo, Egypt.

²King Abdulaziz University, Jeddah, Saudi Arabia.



CrossMark

IN THIS paper, TiO₂ impurities exist in kaolin were investigated for the first time as active centers for photo degradation of M.B (Methylene Blue) dye. The study extends to examine the same impurities after its transformation into NaP zeolite. Simultaneous removal of heavy metals (Pb²⁺, Cu²⁺, Ni²⁺, Co²⁺) in presence of organic dye over metakaolinite phase and NaP zeolite was performed in presence and absence of UV irradiation.

The samples were characterized using XRD, SEM, EDX, Diffuse UV-Vis spectrophotometer and finally drawing the kinetic curves of removal of heavy metal ions and M.B dye. The results showed that the TiO₂ impurities in metakaolinite exists in anatase form and maintain its existence in the transformed NaP zeolite with the same phase. Both NaP and metakaolinite showed photo catalytic activity towards degradation of M.B dye. However, the NaP zeolite showed superior behavior for simultaneous removal of both pollutants with UV Irradiation. Investigation and mode of removal of both samples were investigated.

Keywords: Kaolin, NaP zeolite, Anatase impurities, Photo degradation, Simultaneous removal.

Introduction

Kaolin is a natural clay that exists in many countries around the world [1-5]. Kaolin is becoming a raw material for many industries such as ceramic industries [6]. In addition, metakaolinite or the calcined form kaolin at high temperature [500-800] is the base of cement and ceramic industry [7]. Moreover, kaolin was used in catalyst industry either as, support or a binder for many vital industrial processes such as FCC cracking processes [8]. Furthermore, metakaolinite is used as a raw material for preparation of many types of zeolites [9-15]. Due to the high importance of such clay many governments invest in exploring and magnifying the utilization of such important clay. Thus Saudi Arabia government for example, invests more than 4 M \$ in exploring kaolin in KSA [16].

The use of kaolin as a photo catalyst, however is restricted to be used as a support for photocatalyst sensitive materials such as Ti source [17]. In spite of the fact that Ti may be exit naturally occur in kaolin clay, only few papers deal with the importance of these impurities such as iron, titanium and vanadium [18]. Thus, Tasuma Suzuki et al. evaluate the presence of Ti as anatase form in kaolin in its efficiency for removal of heavy metals and correlate a direct relation between its existence and the efficiency of removal [18].

Moreover, in water pollution, kaolin could be used as it is for adsorption of pollutants or after its transformation into low cost prepared zeolite in order to effectively remove heavy metals [19-22]. The most common low silica zeolite used in this field is LTA, FAU [22]. Low NaP zeolite

*Corresponding author e-mail: ehgazy77@yahoo.com

Received 17/4/2019; Accepted 5/5/2019

DOI: 10.21608/ejchem.2019.12026.1758

© 2019 National Information and Documentation Center (NIDOC)

[Na₆Al₆Si₁₀O₃₂·12H₂O], however, was proven to be more softener for water than most common used LTA zeolite [23].

Although, the zeolite is most common adsorbent used for removal of heavy metals, Many attempts are done to simultaneous removal of organic and inorganic pollutants by mixing two effective adsorbents including zeolite [24] to effectively remove both pollutants simultaneously. Regards to organic pollutants, photo degradation of organic pollutants becomes one of the most effective methods to remove pollutants especially if it is based on local sunlight such as Jeddah sunlight [25].

In this work we will for the first time, investigate the efficiency of tio₂ impurities in metakaolinite phase on photo degradation of organic dyes in presence and absence of inorganic heavy metals. In addition, a comparison study will be done between the metakaolinite phase and na-p transformed phase on the efficiency of simultaneous removal of both pollutants.

Experimental

Materials used

Sodium Hydroxide and kaolin clay. The kaolin clay used in the present investigation was supplied from Azabira site in the north part of Saudi Arabia. Copper nitrate (Cu(NO₃)₂·3H₂O (Sigma-Aldrich), nickel nitrate (Ni(NO₃)₂·6H₂O (Sigma-Aldrich), lead nitrate (Pb(NO₃)₂ (Sigma-Aldrich), Cobalt nitrate (Co(NO₃)₂·6H₂O (Sigma-Aldrich) Methylene blue dye (C₁₆H₁₈ClN₃S·xH₂O) (Sigma-Aldrich) were used.

Preparation of zeolite P from kaolin

Zeolite P was prepared by using simple method. Firstly, the kaolin was calcinated and converted to metakolinite for 6hr at 700°C. 18.45g of Metakolinite was added to sodium hydroxide solution was performed (24 g) dissolved in 184.5 H₂O. After that the reaction mixtures were left for 24hr at room temperature. Then, weight 80.31g of Sodium silicate solution (39%) then added to the above solutions and left for 24hr. The mixture was put in water bath for 7hr at 100°C. Then, the mixture was filtered, washed by distilled water several times and dried at 80°C overnight. The samples were then crushed and collected in containers.

Photocatalytic experiments

A 100mL mixed solution of methylene blue was mixed with 0.1 g of composite using

a horizontal cylinder annular batch reactor. A xenon lamp (300 W), covered by aUV filter, was used for irradiation of the photocatalyst. The photocatalytic reaction was carried out at room temperature. Different amounts of solutions is collected by time for analysis

Synthetic waste water was prepared by 10 PPM of Methylene Blue dye with and without 100 PPM of each heavy metal.

Characterization techniques

XRD (X-ray diffraction analysis)

X-ray diffractograms of samples under investigation were collected using a Bruker D8 advance instrument with a CuKα1 radiation and a secondary monochromator operated at 40 kV and 40 mA. The crystal lattice and space group analysis were performed using a Philips X'Pert Plus V. 1.023 .04. 1999.

SEM and EDX analysis

Scanning electron microscopy (SEM) images of different samples and EDX analysis was performed using a "JXA-840 A Electron Probe Micro Analyzer-Japan"

Diffuse reflectance U.V. Visible spectra

DRUV-vis spectral data was obtained using Thermo-Scientific evolution spectrophotometer equipped with an integrating sphere in the wavelength range of 200–800 nm to measure the reflectance spectra of samples. The Band gap energy values of all investigated samples were calculated using Kubelka-Munk procedure. The Kubelka-Munk factor (K) was determined by following equation; $K=(1-R)^2/2R$

Where R is the % reflectance. The wavelengths (nm) were translated into energies (E) and a plot was drawn between $(K^*E)^{0.5}$ and E to obtain a curve. The bandgap energy (eV) was obtained as the intersection point of the two slopes in the curve. [25].

Results and Discussions

XRD (X-ray diffraction)

XRD diffraction patterns of Calcinedkaolin and Na-P zeolite are given in Fig. 1. The phase analysis showed that the calcined kaolin is decomposed and no trace for the kaolinite structure. Thus, only anatase phase is appeared in the diffraction patterns which originally exists in the crude kaolin. After hydrothermal treatment Na-P zeolite is observed with a pure phase. Small quartz single sharp signal is appeared which is

common in zeolitization process from kaolin [26]. In addition, the anatase phase still exists in the structure with nearly 95% of its original intensity in calcined kaolin (Table 1).

Scanning Electron Microscope (SEM) and EDX analysis

SEM images of calcined kaolin and Na-P zeolite are given in Fig. 2. It is clear observed that, calcined kaolin showed amorphous matrix without appearance of any crystal structure as expected from calcination of kaolin and its transformation into metakaolinite amorphous phase [2]. Moreover, clear tetragonal crystals of Na-P zeolite appeared in SEM image. The tetragonal shape of Na-P zeolite is accumulated to form a spherical shape however, the tetragonal shape is still could be differentiated from SEM image. This phenomenon

is common in the zeolitization process that occurs from natural clay [27].

In addition, EDX analysis is given in Table 2 showed that TiO_2 exists in about 1.5 wt% in calcined kaolin which confirmed as anatase phase before from XRD. The TiO_2 still exists incrystallized Na-P zeolite but with less amount about 1.23wt%. The decrease in the TiO_2 amount in the zeolite sample may be due to the loss of TiO_2 during the hydrothermal treatment.

Diffuse reflectance (DR)

Diffuse reflectance spectra of calcined kaolin samples and Na-P zeolite are given in Fig. 3. The band gap of each sample is calculated. The values of band gaps are similar to that of anatase phase and is around 3.2 e.v which reflects the presence

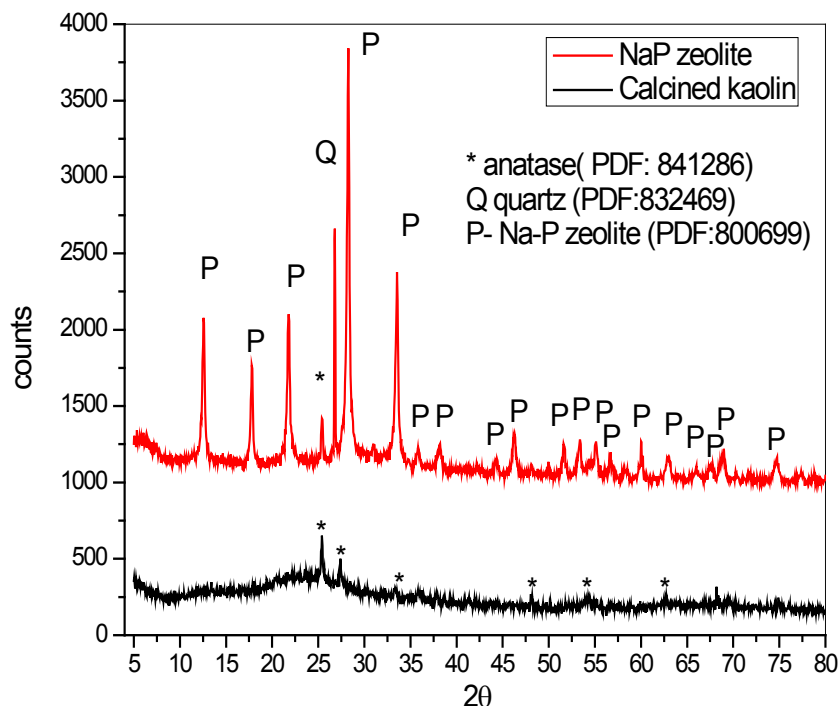


Fig. 1. XRD patterns of Calcined kaolin and Na-P zeolite.

TABLE 1. Crystal lattice analysis of Na-P zeolite and calcined kaolin.

Sample	Lattice parameters						V/10 ⁶ pm ³	Max peak Height	
	a	b	c	a	b	g		P zeolite	Anatase
Na-P	9.988	9.988	5.016	90	90	90	500	2671	291
Calcined kaolin									308

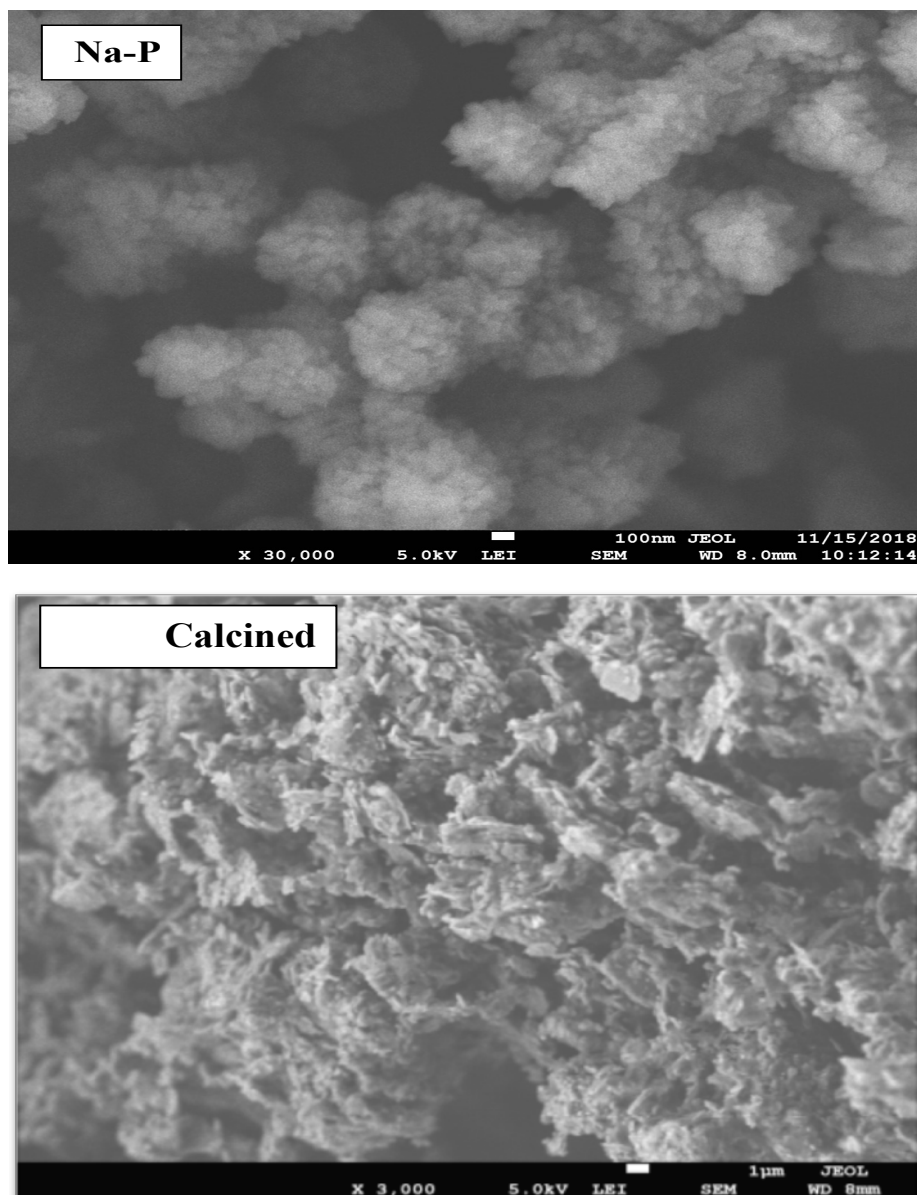


Fig.2. SEM images of calcined kaolin and Na-P zeolite.

TABLE 2. EDX analysis of prepared samples.

Element	Calcined kaolin	NaP
	Wt%	
O	48.23	57.98
Al	23.70	11.44
Si	26.12	20.08
Ti	1.47	1.23
Na	0.49	9.27

of anatase phase inside either the calcined kaolin sample and the corresponding prepared Na-P zeolite.

Photo catalytic activity of prepared samples

Egypt.J.Chem. **62**, No. 11 (2019)

Photo catalytic activity of calcined kaolin sample and Na-P prepared zeolite was examined in degradation of M.B dye. In order, to complete evaluation, the kinetic curves were drawn with and without photo irradiation. In addition, it is

also performed in presence and absence of 400 PPM of heavy metal ions (Pb, Cu, Co, Ni); 100 PPM of each.

Figure 4 showed the degradation kinetic curves of all above cases. From this figure, it could be observed that both kaolin and Na-P zeolite samples have a considerable capacity for adsorption of M.B dye. However, this capacity, as expected, is enlarged considerably when calcined kaolin is converted to the corresponding Na-P zeolite with three dimensional porous structure and high surface area. Although, the mode of adsorption exists, when samples are irradiated an increase in the amount of dye removal is observed which emphasizes that both calcined kaolin and corresponding Na-P zeolite has more or less photo catalytic activity which is expected from XRD patterns before due to presence of anatase phase within both structures. In absence of ions, it seemed that, the total amount of dye removed

by either adsorption or irradiation is preferred to Na-P zeolite reaches about 80% removal without irradiation and about 90% removal upon irradiation. While, maximum amount of removal by calcined kaolin did not exceed 50% with irradiation. Although that, the difference between removal % of irradiated and non irradiated samples is much higher for calcined kaolin while, it seemed to be very small for Na-P zeolite. This could be explained by that, the photo degradation mode is much higher in calcined kaolin sample than that of Na-P sample while, adsorption mode in Na-P sample is much higher than that of calcined kaolin sample.

A dramatic change in this behavior was observed when 400 PPM of heavy metal ions is introduced in solution combined with 10 PPM M.B Dye.

Thus, in presence of ions, more inhibition of

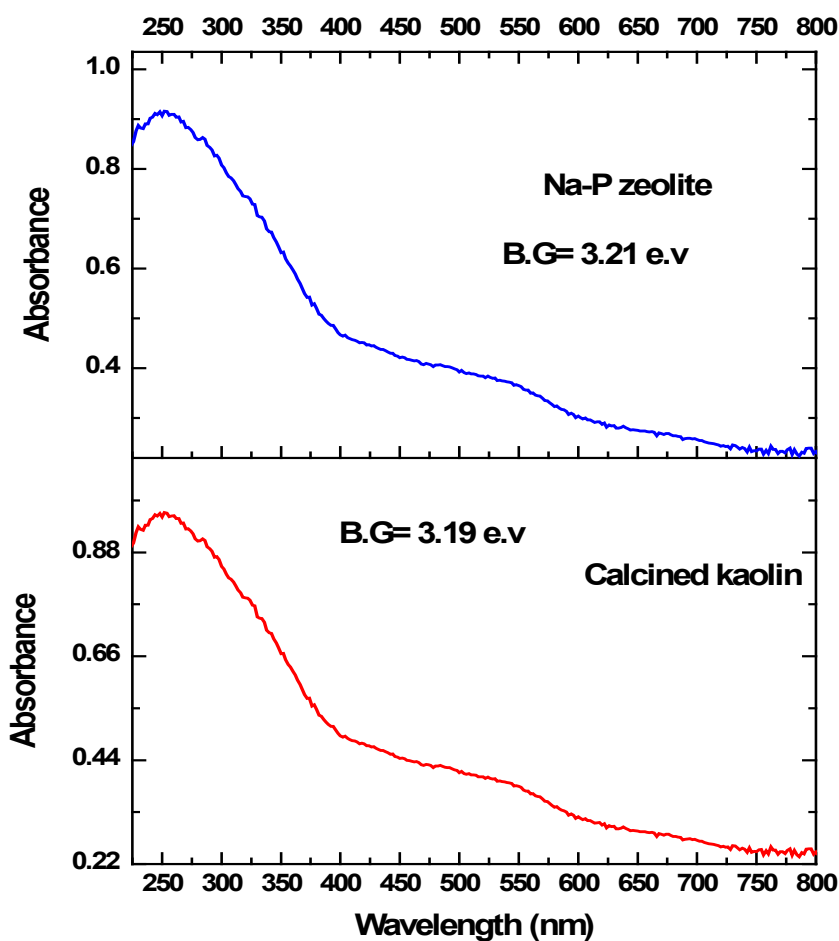


Fig. 3. Diffuse reflectance spectra of calcined kaolin and prepared zeolite samples.

both modes of removals was observed for calcined kaolin sample reaches only 10% removal with irradiation. In contrary, Na-P samples showed only inhibition in adsorption mode, while photo degradation mode is enlarged to achieve about 60% removal with irradiation.

Removal of heavy metals ions in presence of dye

In order to take a look about the removal behavior of both samples towards ions, kinetics curves of removal of ions individually (Fig. 5) and totally (Fig. 6) with and without irradiation is figured. In contrary to dye, ions are only

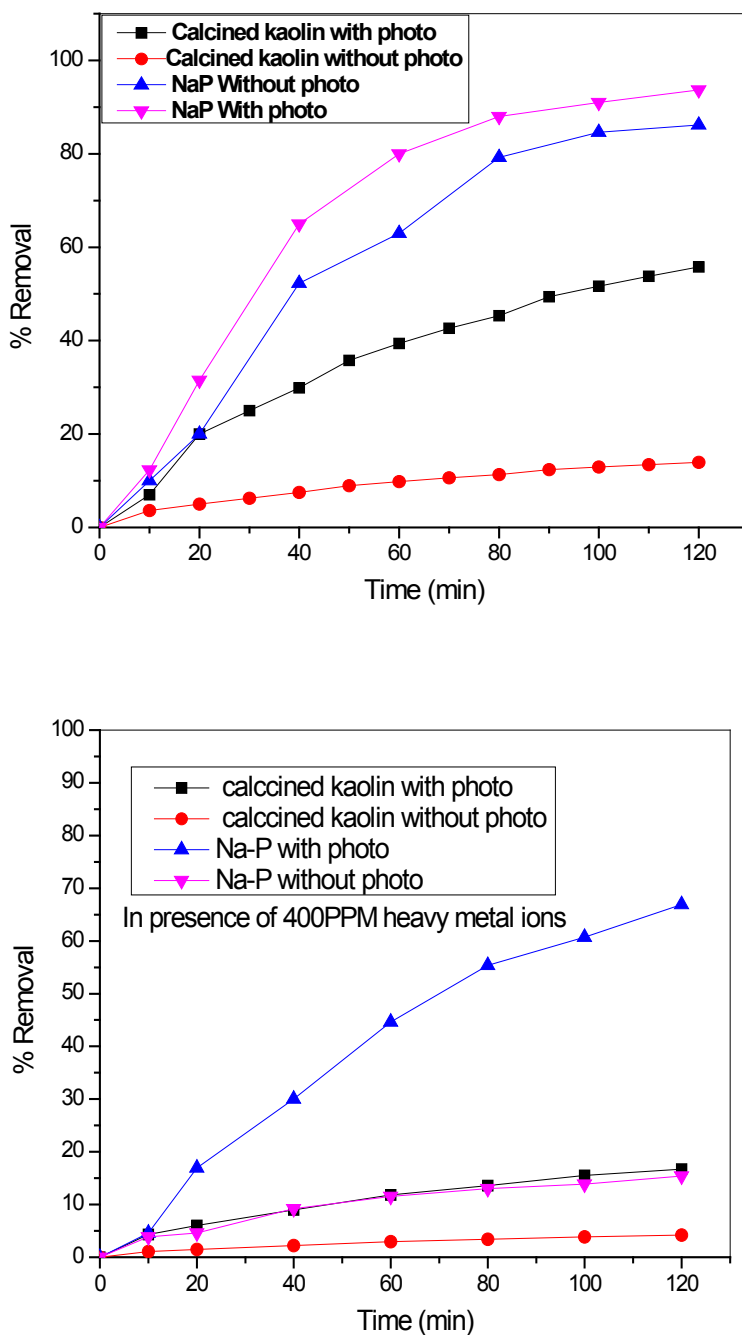


Fig. 4. Photo degradation kinetic curve of 10 PPM dye of M.B, with and without photo irradiation and in presence and absence of heavy metal ions.

removed by adsorption and/or ion exchange mode. However, the presence of degradation process may affect the removal of ions as will be seen. Thus from Fig. 6, it could be observed that, the removal capacity of ions for calcined kaolin is very limited reaches only less than 10 % either with or without irradiation. While, the Na-P zeolite have a large capacity towards ions reaches about more than 60% removal. The behavior of Na-P zeolite samples is time affected by irradiation that, irradiation reduces the removal capacity for the time of 0-60 min. after which the capacities are nearly equal. In order to explore the selectivity and partial capacities of ions,

individual kinetic curves of ions are figured in Fig. 5. From these figures it could be observed that, as a general observation, the selectivity of Na-P towards $Pb^{2+} > Cu^{2+} >>>> Ni^{2+} > Co^{2+}$. Moreover, irradiation affects the partial capacities of Na-P zeolite towards Pb^{2+} and Cu^{2+} at time of 0-<80min after which the two lines are superimposed. Co^{2+} and Ni^{2+} ions are seemed to be less effected by irradiation.

Photo catalytic activity per TiO_2 active centre

In order to deeply understand the mode of photo catalytic activity of TiO_2 active centers exists in either calcined kaolin or Na-P zeolite,

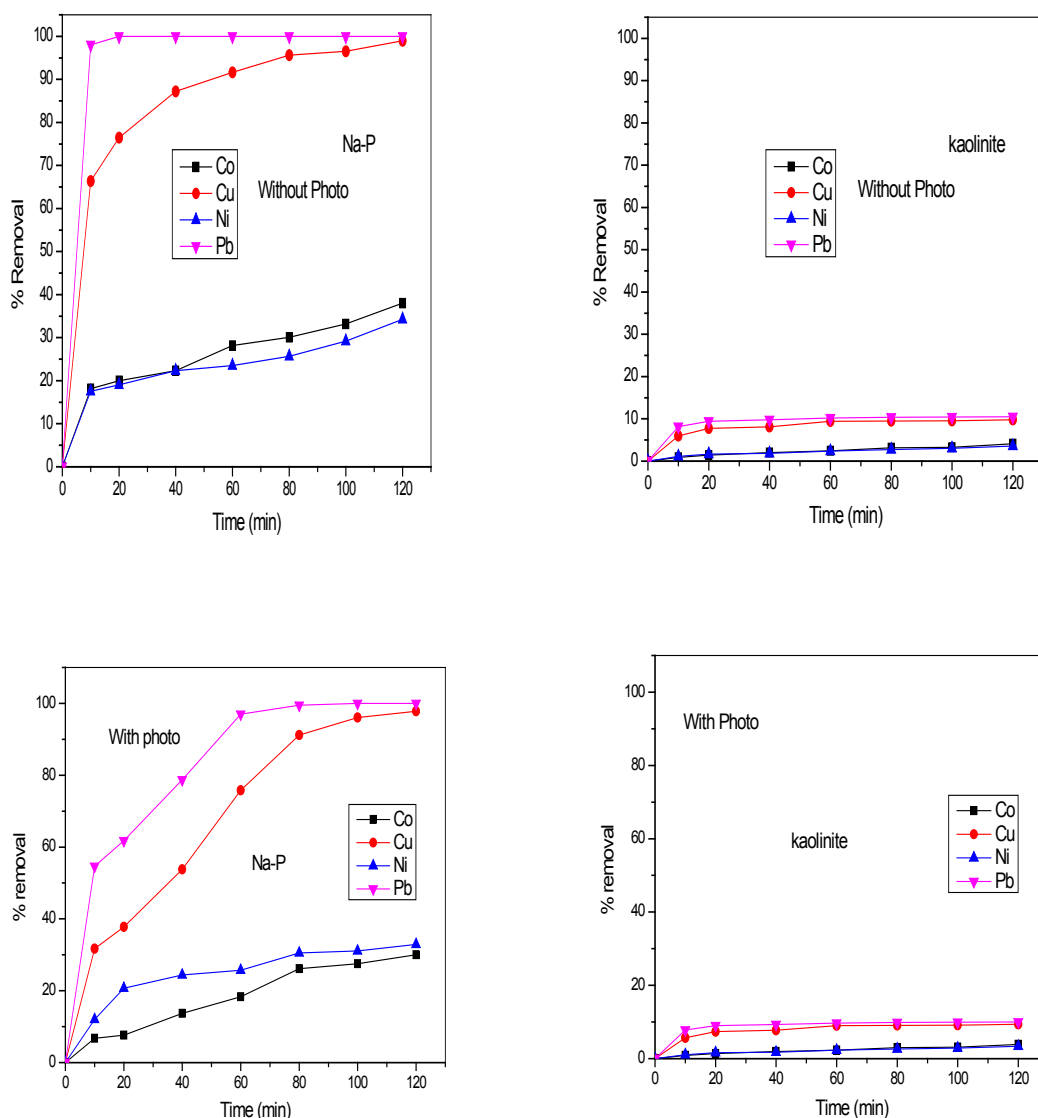


Fig. 5. kinetic curves of removal of Pb^{2+} , Co^{2+} , Cu^{2+} , Ni^{2+} over samples with and without irradiation.

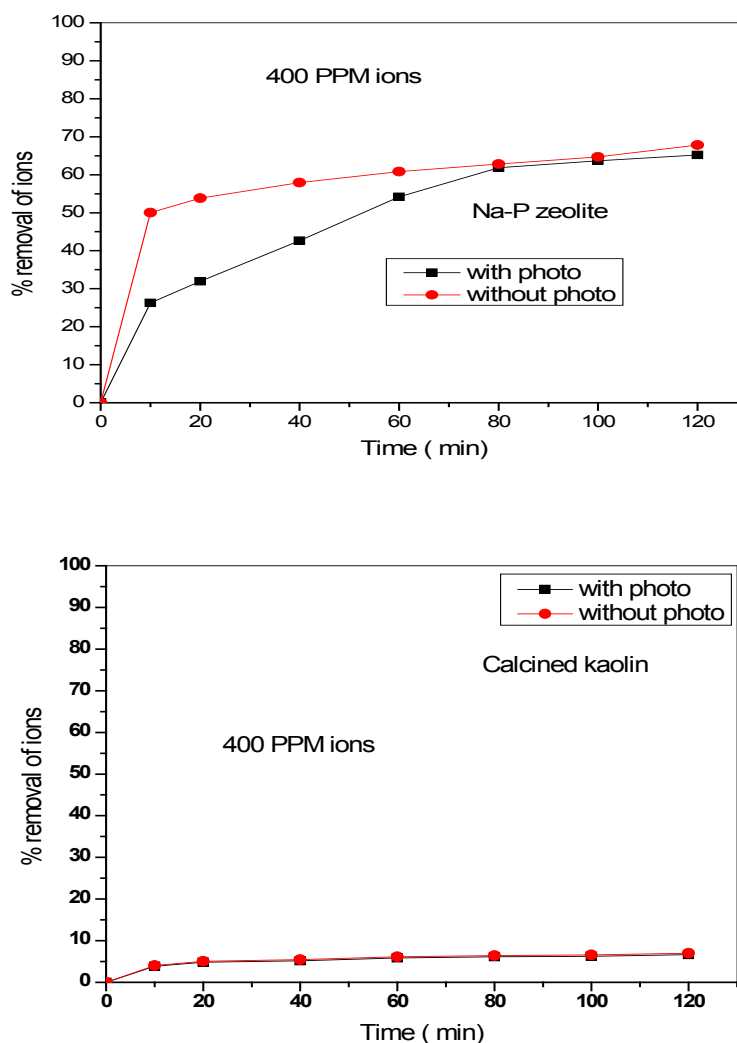


Fig. 6. kinetic curves of the sum of all ions removal over samples with and without irradiation.

isolation of two modes of removal (adsorption ; photo degradation) should be performed. Thus could be happened by subtract two kinetic curves of irradiated and non irradiated samples followed by division on the amount of TiO_2 (calculated from EDX analysis) of each sample. This will resulted in the photo catalytic activity of sample per wt% of TiO_2 , which could be less complicated than the study of both modes of removal together. Figure 7 showed the photo catalytic activity per Wt% TiO_2 against time for all samples in absence and in presence of ions.

From this figure it could be observed that the TiO_2 active centers in calcined kaolin is inhibited by the presence of ions decreased from 25 to only 5. While, in contrary, the TiO_2 active centers in

Na-P zeolite is enhanced by the presence of ions thus it increases from 15 to 40. In addition, this increase is not linear with time, thus after nearly 40 min, a non linear increase is observed. This could explain why the partial capacity of ions at lower time is decreased upon irradiation and then again increases at higher times. Thus at lower time, the mode of adsorption for both dye and ions becomes predominant which means a competition between dye and ions for the same active adsorption sites. While after considerable time 40-60 min, the TiO_2 centers become photo catalytically active and the degradation of dye is predominant which leaves the adsorbed site for ions, increasing the capacity for ions again.

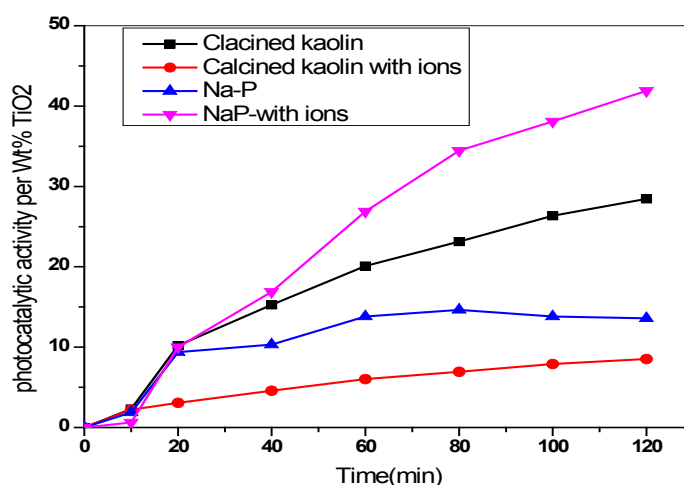


Fig. 7. Photo catalytic activity per wt% TiO₂ for all investigated sample with and without irradiation.

Conclusions

From the above study, the following conclusion could be drawn:

1. Anatase phase impurities in metakaolin were examined for the first time as photoactive centers for degradations of organic pollutants.
2. Hydrothermal transformation of metakaolin into Na-P zeolite maintains nearly the same amount of anatase phase impurities.
3. The photo degradation behavior of zeolite prepared from kaolin with such impurities in addition to the high ion exchange capability of zeolite enables it to act as a dual removal adsorbent for both heavy metals and organic Dye under UV irradiation.
4. The use of low cost clay such as kaolin in preparation such dual removal adsorbent magnify the economic use of such prepared materials.

Acknowledgement

This work was funded by the king Abdulaziz City for Science and Technology (KACST), Under Grant no. 0032-009-01-17-1. The authors, therefore, acknowledge with thanks the KASCT for technical and financial support.

References

1. C. Lopes, V. Lisboa, J. Carvalho, A. Mateus, L. Martins, Challenges to access and safeguard mineral resources for society: A case study of kaolin in Portugal, *Land Use Policy*, **79**, 263-284 (2018).
2. Robert J. Pruett, Kaolin deposits and their uses: Northern Brazil and Georgia, USA, *Applied Clay Science*, **131**, 3-13 (2016), ISSN 0169-1317
3. GemechuBedassa, WorashGetaneh, BinyamHailu, Geochemical and mineralogical evidence for the supergene origin of kaolin deposits – Central Main Ethiopian Rift, *Journal of African Earth Sciences*, **149**, 143-153 (2019).
4. Mahmoud E. Awad, RedaAmer, Alberto López-Galindo, Mahmoud M. El-Rahmany, Luis F. García del Moral, César Viseras, Hyperspectral remote sensing for mapping and detection of Egyptian kaolin quality, *Applied Clay Science*, **160**, 249-262 (2018).
5. Emilio Galán, Patricia Aparicio, Juan Carlos Fernández-Caliani, Adolfo Miras, Marcial G. Márquez, Anthony E. Fallick, Norbert Clauer, New insights on mineralogy and genesis of kaolin deposits: The Burela kaolin deposit (Northwestern Spain), *Applied Clay Science*, **131**, 14-26 (2016).
6. SitiKhadijah Hubadillah, Mohd Hafiz Dzarfan Othman, Takeshi Matsuura, A.F. Ismail, Mukhlis A. Rahman, Zawati Harun, Juhana Jaafar, Mikihiro Nomura, Fabrications and applications of low cost ceramic membrane from kaolin: A comprehensive review, *Ceramics International*, **44**(5), 4538-4560 (2018).
7. Enas Muhi Hadi, Sahar Issa Hussein, A sustainable method for Porous refractory ceramic Manufacturing from kaolin by adding of burned *Egypt. J. Chem.* **62**, No. 11 (2019)

- and raw wheat straw, *Energy Procedia*, **157**, 241-253 (2019).
8. Hui Wang, Hongfei Lin, Ying Zheng, Siau Ng, Hilary Brown, Yu Xia, Kaolin-based catalyst as a triglyceride FCC upgrading catalyst with high deoxygenation, mild cracking, and low dehydrogenation performances, *Catalysis Today*, **319**, 164-171 (2019).
 9. MousaGougazeh, J.-Ch. Buhl, Synthesis and characterization of zeolite A by hydrothermal transformation of natural Jordanian kaolin, *Journal of the Association of Arab Universities for Basic and Applied Sciences*, **15**, 35-42 (2014).
 10. Lijalem Ayele, Joaquín Pérez-Pariente, Yonas Chebude, Isabel Díaz, Conventional versus alkali fusion synthesis of zeolite A from low grade kaolin, *Applied Clay Science*, **132–133**, 485-490 (2016).
 11. Djoko Hartanto, Riskaviana Kurniawati, Agung Bagus Pambudi, Wahyu PrasetyoUtomo, Wai Loon Leaw, HadiNur, One-pot non-template synthesis of hierarchical ZSM-5 from kaolin source, *Solid State Sciences*, **87**, 150-154 (2019).
 12. Jing-Quan Wang, Ya-Xi Huang, Yuanming Pan, Jin-Xiao Mi, Hydrothermal synthesis of high purity zeolite A from natural kaolin without calcination, *Microporous and Mesoporous Materials*, **199**, 50-56 (2014).
 13. Lijalem Ayele, Joaquín Pérez-Pariente, Yonas Chebude, Isabel Díaz, Synthesis of zeolite A from Ethiopian kaolin, *Microporous and Mesoporous Materials*, **215**, 29-36 (2015).
 14. Jing-Quan Wang, Ya-Xi Huang, Yuanming Pan, Jin-Xiao Mi, New hydrothermal route for the synthesis of high purity nanoparticles of zeolite Y from kaolin and quartz, *Microporous and Mesoporous Materials*, **232**, 77-85 (2016).
 15. Yunan Ma, Chunjie Yan, ArefAlshameri, XiumeiQiu, Chunyu Zhou, Dan li, Synthesis and characterization of 13X zeolite from low-grade natural kaolin, *Advanced Powder Technology*, **25** (2), 495-499 (2014).
 16. Saudi Arabia: Ma'aden – kaolin, Focus on Pigments, **2007**, (7), (2007), Page 6, ISSN 0969-6210, [https://doi.org/10.1016/S0969-6210\(07\)70207-2](https://doi.org/10.1016/S0969-6210(07)70207-2).
 17. Yahya N., Aziz F., Jamaludin N.A., Mutalib M. A., Ismail A.F., Salleh W.N.W., Jaafar J., Yusof N., Ludin N. A., A review of integrated photocatalyst adsorbents for wastewater treatment, *Journal of Environmental Chemical Engineering*, **6** (6), 7411-7425 (2018).
 18. Tasuma Suzukia,b,* , KisyoNakasec, Satoshi Kakoyamac, Junko Takamurod, MiyuOkitad, Masakazu Niinaea, The role of anatase impurity in the leaching of Cd(II) from contaminated kaolinite, *Journal of Environmental Chemical Engineering* **7**, 102851 (2019).
 19. Shamsan S. Obaid, D.K. Gaikwad, M.I. Sayyed, Khader AL-Rashdi, P.P. Pawar, Heavy metal ions removal from waste water by the natural zeolites, *Materials Today: Proceedings*, **5**(9), Part 3, 17930-17934 (2018).
 20. Mei Hong, Lingyun Yu, Yanding Wang, Jian Zhang, Zhuwen Chen, Lei Dong, QijieZan, Ruili Li, Heavy metal adsorption with zeolites: The role of hierarchical pore architecture, *Chemical Engineering Journal*, **359**, 363-372 (2019).
 21. Zhanchao Li, Lijie Wu, Shuang Sun, JunliGao, Hanqi Zhang, Zhiquan Zhang, Ziming Wang, Disinfection and removal performance for Escherichia coli, toxic heavy metals and arsenic by wood vinegar-modified zeolite, *Ecotoxicology and Environmental Safety*, **174**, 129-136 (2019).
 22. Eman Z. Hegazy, Islam H. Abdelmaksod, Samia A. Kosa, Removal of heavy metal quaternary cations systems on zeolite A and X mixtures prepared from local kaolin, *CLEAN–Soil, Air, Water* **42** (6), 775-778 (2014).
 23. Christopher J. Adams, Abraham Araya, Karen J. Cunningham, Kevin R. Franklin and Ian F. White , Measurement and prediction of Ca–Na ion-exchangeequilibrium in maximum aluminium P (MAP), a zeolite with the GISframework topology, *J. Chem. Soc., Faraday Trans.*, **93**, 499-503 (1997).
 24. Islam HamdyAbd El Maksod, Elham A. Elzaharany, Samia A. Kosa, Eman Z. Hegazy, Simulation program for zeolite A and X with an active carbon composite as an effective adsorbent for organic and inorganic pollutants, *Microporous and Mesoporous Materials*, **224**, 89-94 (2016).
 25. Islam Hamdy Abd El Maksod, Abdelmohsen Al-Shehri, Salem Bawaked, Mohamed Mokhtar, KatabathiniNarasimharao, Structural and photocatalytic properties of precious metals modified TiO₂-BEA zeolite composites, *Molecular Catalysis*, **441**, 140-149 (2017).
 26. LM Al-Harbi, SA Kosa, IH Maksod, EZ Hegazy, The photocatalytic activity of TiO₂-Zeolite composite for degradation of dye using synthetic

-
- UV and Jeddah sunlight, *Journal of Nanomaterials* **16** (1), 46 (2014).
27. Characterization of some zeolites prepared from local materials, IHA El-Maksoud, *M. Sc. Thesis*, Cairo University (2002).
28. Eman Z. Hegazy, Samia A. Kosa, Islam Hamdy Abd El Maksod, Synthesis and characterization of JBW structure and its thermal transformation, *Journal of Solid State Chemistry*, **196**, 150-156 (2012).